Modified Raman confinement model for Si nanocrystals

Giuseppe Faraci,* Santo Gibilisco, Paola Russo, and Agata R. Pennisi
Dipartimento di Fisica e Astronomia, Universitá di Catania; MATIS-Istituto Nazionale di Fisica della Materia, Via Santa Sofia 64, 95123 Catania, Italy

Salvo La Rosa
Elettra, Sincrotrone Trieste, Trieste, Italy

(Received 25 May 2005; revised manuscript received 8 November 2005; published 10 January 2006)

A modified one-phonon confinement model is developed for the calculation of micro-Raman spectra in Si nanocrystals, permitting the simultaneous determination of the Raman frequency, intensity, and linewidth. Using a specific spatial correlation function and the Si phonon dispersion relations, the Raman spectra are calculated under the limitations imposed on the wave vector by the spatial confinement. Results are obtained as a function of the Si nanocrystal size in the range 1.2–100 nm. The frequency shift and line broadening of the Raman spectra are compared with experimental results reported in the literature.

DOI: 10.1103/PhysRevB.73.033307 PACS number(s): 78.67.Bf, 36.20.Ng, 61.46.−w, 78.30.Am

The optical properties of Si quantum dots are, at present, deeply investigated for their potential technological applications. Of course, a great effort is dedicated to the interpretation of the experimental results, related to quantum confinement effects, in the light of current theories developed for specific cases. Among the various investigation techniques, Raman spectroscopy is a very sensitive tool for probing semiconductor nanostructures and in particular Si quantum dots (QD's) in the nanometer range.[1–18] Here, the vibrational properties of the nanostructures—i.e., the acoustic and optical phonon modes in confined systems—and the interaction with a photon and the modification of selection rules play a fundamental role for the understanding of a basic scattering process with a short wave vector.

From an experimental point of view, with reference, e.g., to the specific case of Si bulk crystal, the Raman spectrum exhibits a peak at 521 cm^{-1} due to the optical phonon dispersion curves, with a linewidth Γ. In nanocrystals, valuable experimental information can be obtained by Raman spectroscopy, as a function of the size, through the energy shift of the Raman peak and the correspondent line broadening, both size dependent.

In order to obtain a good interpretation of these experimental data, several models have been developed. Among them we recall the microscopic force model,[5] the bond polarization model,[6,7] and the spatial correlation model;[16] in some cases, phenomenological approachs, considering optical and/or acoustic phonons, have been attempted.[3,4,17]

However, none of these models gives a satisfactory description of the phonon confinement within the dot, capable of determining simultaneously the frequency shift and the linewidth. Furthermore, poor agreement between experimental data and theoretical calculations has been obtained,[11] although some phenomenological theory can give the qualitative trend of the Raman shift as a function of the size, using *ad hoc* confinement phonon functions. In the literature, spatial correlation models which use arbitrary confinement functions such as Gaussian,[17] exponential,[4,15–17] and sine functions[3,6,17] have been adopted, without any justification concerning the possible phonon wave vectors and their distribution in the dot.

We recall that the momentum selection rule $q=0$ of first-order Raman spectra of bulk crystals is violated for nanodots because of the strong size confinement. This implies a great care in the superposition of possible phonon wave vectors, which play an important role not only in the wave function of the confined system but also in the integration limits of the final Raman spectrum.

In the present study we criticize some of the assumptions of current Raman spatial correlation theories for semiconductor nanocrystals. In particular, for Si QD's, we develop an improved expression for the Raman spectrum, allowing the determination of the frequency shift and of the line broadening, as a function of the QD size. Moreover, the optical phonon Raman scattering is investigated; finally, we compare the present theory with some of the previous models and with current experimental results.

In a perfect crystal the first-order Raman scattering of a photon selects contributions of phonons obeying the equation $\mathbf{q}\approx 0$ ($\mathbf{q}$ being the phonon wave vector), because of the momentum conservation law. Therefore, this selection rule implies the contributions of phonons at the center of the Brillouin zone. However, when the size of the crystal is quite limited, the previous rule $\mathbf{q}\approx 0$ is no longer valid. Consequently, the Raman spectrum is calculated[3,17] by the following integral over the momentum vector $\mathbf{q}$:

$$I(\omega)\propto[n(\omega)+1]\int |C(\mathbf{q})|^2 L(\omega,\mathbf{q})d\mathbf{q},$$

where the integral is extended to the entire first Brillouin zone, ω is the Raman frequency, $n+1$ is the Bose-Einstein factor, $C(\mathbf{q})$ are Fourier coefficients of the phonon wave function, and $L(\omega,\mathbf{q})$ is the Lorentzian function related to the phonon dispersion curve $\omega'(\mathbf{q})$, with a natural Lorentzian line shape Γ.

The following questions now arise.

(i) Which phonon wave vectors are possible in a QD and how is the phonon spectrum modified?

(ii) Of the possible phonon wave vectors, which are contributing to the scattering process and with which probability distribution?

(iii) How should the Raman spectrum be calculated and is an integration range extended over the entire Brillouin zone still correct?

These are very critical points. In a linear vibrating string of length D the possible wave vectors of confined phonons can be assumed[19] as $\mathbf{k}_n = n\pi/D$, with wave functions requiring a vanishing vibrational amplitude at the border. Of course, in a QD a simple picture of parallel vibrating planes with boundaries at the QD border is oversimplified; short- and long-range interactions, surface effects, bond length, and bond angles[5] are important in a microscopic treatment. In some models this difficult task was overcome[6,10,17] using a *confinement* function $F_c(r,D)$ in the real space with an arbitrary choice of analytical forms instead. The Fourier transform (FT) of $F_c(r,D)$, i.e.,

$$C(\mathbf{q}) = \frac{1}{(2\pi)^3} \int F_c(\mathbf{r},D)\exp(-i\mathbf{q}\cdot\mathbf{r})d^3r,$$

was assumed as the phonon amplitude in the nanocrystal—i.e., as a superposition of plane-wave eigenfunctions with $\mathbf{q}$ wave vectors; the final Raman spectrum in the dot was therefore written as

$$I(\omega) \propto \int_0^{2\pi/a} \frac{|C(\mathbf{q})|^2 d\mathbf{q}}{[\omega - \omega'(\mathbf{q})]^2 + (\Gamma/2)^2},$$

where the limits of the integral were extended to the Brillouin zone (a being the Si lattice parameter $a=0.543$ nm).

We modify the previous approach, observing that a function $F_c(r,D)$ actually corresponds to a single-phonon wave vector, which is not realistic. We should instead have a wave packet extended over the QD size, with a spread $\Delta r \approx D$ in real space and $\Delta q \approx 1/D$ in $\mathbf{q}$ space according to the Heisenberg uncertainty principle.

In our approach we assume the phonon wave function in a dot as a weighted superposition of sinusoidal waves with $\mathbf{k}_n = n\pi/D$, $n=2,4,6\ldots n_{\max}$ ($n_{\max}$ is equal to the maximum integer smaller than $2D/a$):

$$F_c(r,D) = \sum_n \frac{\sin(k_n r)}{k_n r}, \quad \text{for } r \leqslant D/2, \text{ or 0 otherwise.}$$

This is justified by the following considerations.

(1) The wave vectors are consistent with the vibrational behavior of a linear vibrating atomic chain of length D, where D should be a multiple of the wavelength λ.

(2) The function $F_c(r,D)$ has components centered at $r=0$, strongly decaying and going to zero at the QD border; note that this annulation at the QD border excludes even values of n.

(3) As shown in Ref. 6 for a Si cluster with $D=2.35$ nm, the first component of $F_c(r,D)$ is the most appropriate for simulating the vibrational amplitude of the most Raman-active modes in a Si QD.

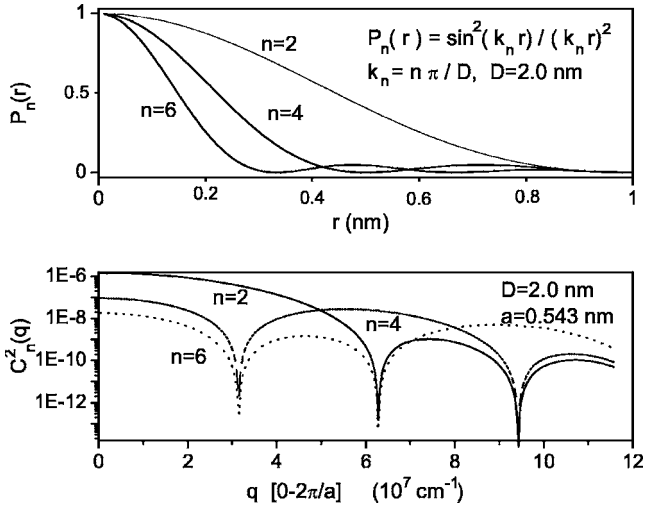

FIG. 1. Upper plot: probability distribution $P_n(r)$ as a function of the radial distance r from the dot center of some components of the phonon wave function. These distributions go to zero at the dot border and have their maximum at the center. Lower plot: confinement coefficients in logarithmic scale for a few values of n as a function of $\mathbf{q}$.

(4) The function $F_c(r,D)$ implies probability distributions (see Fig. 1) as a function of r depending on $\mathbf{k}_n$.

(5) The Fourier transform of $F_c(r,D)$ gives the probability amplitude of the phonon contribution with a value $\mathbf{q}$ in the range $(n\pi-1)/D$, $(n\pi+1)/D$, as imposed by the Heisenberg uncertainty principle. This means that a phonon with an initial wave vector $\mathbf{k}_n$ can contribute to the photon scattering process with an effective wave vector $\mathbf{q}$ with the spread allowed by the Heisenberg uncertainty principle around the initial value of $\mathbf{k}_n$. The adimensional FT of each component of $F_c(r,D)$ is

$$C_n(\mathbf{q}) = 3\frac{\sin(qD/2)}{\pi^3 D^3 q(k_n^2 - q^2)}.$$

According to the previous remarks, we calculate the Raman spectrum as

$$I(\omega) \propto \sum_n \int_{(n\pi-1)/D}^{(n\pi+1)/D} \frac{C_n^2(\mathbf{q})d\mathbf{q}}{[\omega - \omega'(\mathbf{q})]^2 + (\Gamma/2)^2},$$

where Γ is the natural Lorentzian line shape, including the instrumental resolution, and the phonon dispersion curve $[\omega'(\mathbf{q})]^2$ adopts the analytical form of Ref. 20: $[\omega'(\mathbf{q})]^2 = A + B\cos(a\mathbf{q}/4)$ with $\mathbf{q}$ in the range 0, $2\pi/a$, $A=1.714\times10^5$ cm^{-2}, $B=1.00\times10^5$ cm^{-2}.

A similar expression is reported by Paillard *et al.*[3] for the average optical phonons in bulk silicon, in the $\mathbf{q}$ range $0-\pi/a$:

$$[\omega'(\mathbf{q})]^2 = 522^2 - \frac{126100q^2}{q+0.53}.$$

Notwithstanding the apparent different analytical form, the phonon dispersion curves look very close to each other in the common range of interest; of course, these dispersion

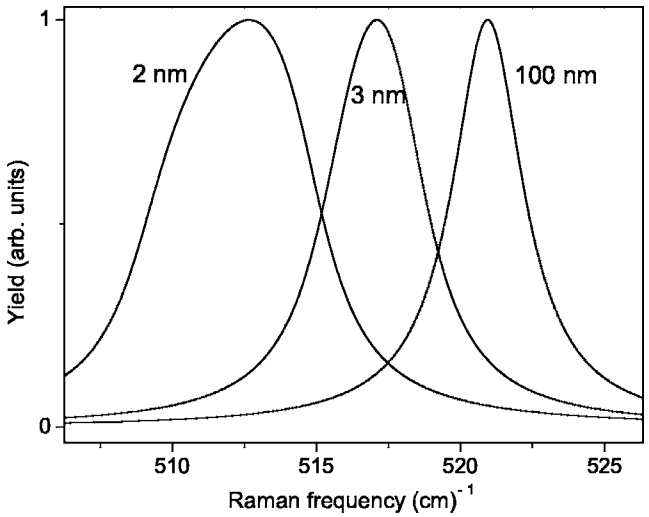

FIG. 2. Calculated Raman spectrum according to the present theory; for each plot the QD size is indicated; the spectra are normalized to the same height, taken equal to unity. The natural linewidth full width at half maximum (FWHM) $\Gamma=3.0$ nm

curves, determined for bulk silicon, are assumed to be valid also for Si nanocrystals.

In Fig. 1 we also plot the confinement coefficients, $C_n^2(\mathbf{q})$, for $n=2,4,6$; note the logarithmic scale and the fast decrease of the coefficients with $\mathbf{q}$.

With the previous assumptions, Raman spectra have been calculated as a function of the QD size; we obtain both frequency shift and line broadening size dependent.

In Fig. 2 we display the Raman curve calculated according to our assumptions for three sizes. At D=100 nm the peak is not shifted at all and presents the natural width (3 cm^{-1}); at lower size, the curve shifts and broadens. In Fig. 3 we synthesize the Raman frequency redshifts for QD diameters in the range 1.2–100 nm. In the same figure, some data reprinted from the literature are reported. For comparison, the bond polarizability (BP) model and the Richter (RWL) model are plotted using their analytical forms:[3]

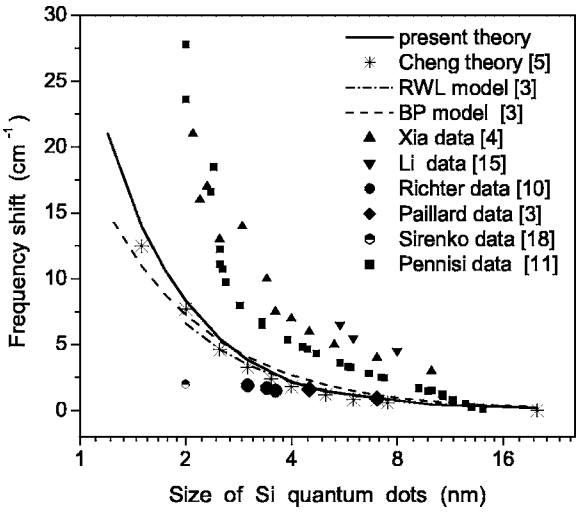

FIG. 3. Plot of the Raman frequency redshift as a function of the QD size, according to the present model. Also reported are the BP model and the RWL model. Experimental data from several authors are displayed for comparison.

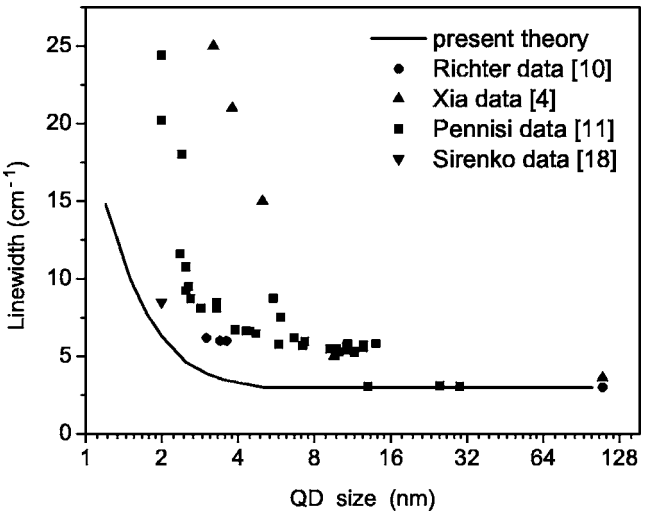

FIG. 4. Plot of the Raman linewidth, as a function of the QD size, according to the present model. The natural linewidth FWHM $\Gamma=3.0$ nm. Experimental values from the literature are displayed for comparison.

$$\Delta\omega = -\beta(a/D)^{\gamma},$$

where $\Delta\omega$ indicates the Raman frequency shift, a is the Si lattice parameter ($a=0.543$ nm), and D is the cluster diameter, whereas β and γ are the following parameters: (i) for the Richter model $\beta=52.3$ cm^{-1} and $\gamma=1.586$; (ii) for the bond polarization model $\beta=47.41$ cm^{-1} and $\gamma=1.44$.

We observe the close agreement at large sizes between all the models and the experiments; at low sizes, however, the experimental data show a shift higher than the calculated one, with a rapid increase around 2–3 nm. Of course, the large scatter of the experimental data for the Raman frequency redshift does not allow a definitive conclusion as regards the comparison of the theoretical approaches with the experiments. In fact, only single-size QD data could indicate whether the phonon dispersion curve and/or the phonon wave function should be refined. In any case the present model is close enough to the data, which could be also affected by surface effects.[4]

As stated above, whereas the current theories are limited to the shift calculation, our expression permits us to calculate also the linewidth of the Raman spectrum. Here, only the broadening due to the limited size is included with the natural width, while the experimental size spread can be eventually taken into account by an average over the correspondent sizes.

In Fig. 4 the line broadening is displayed as a function of the size; an instrumental linewidth FWHM of 3.0 cm^{-1} is assumed; this is the minimum width presented by the Raman curve at large cluster size. We observe also that a higher instrumental resolution would raise the calculated curve accordingly, with a minor influence on the curve shape. In Fig. 4, the data reported in the literature are also reproduced.

We now briefly discuss the results obtained as outlined above. We note the better agreement of our calculations with the experimental results in comparison to similar models. Of course the experimental data are affected by a size spread not included in the theory. This size broadening influences both the redshift and the linewidth as it corresponds to a wide average over some calculated curves. In any case the present model is able, for the first time, to extract from the formulas two parameters such as the Raman shift and the peak width, giving quite a good trend which is very close to the one experimentally obtained. It should be stressed that the experiments could include possible contributions from nanostructures of arbitrary shape and/or strained bonds and surface-enhanced broader agglomerates with substoichiometric oxide;[11,21,22] for such reasons some data can present a shift and width larger than the calculated ones. The present calculations can be also used to deduce the absolute intensity of the Raman features for each QD size. Unfortunately the experiments, being performed on deposited clusters, usually cannot obtain a uniform layer of well-known thickness and controlled size spread. For this reason experimental intensities cannot be compared with each other, and here, we only mention this further information, although it can be easily extracted by our formulas. A final remark should be dedicated to the Raman peak shape, which appears so asymmetric, mainly at small sizes, that it could be possible to distinguish a right linewidth from a larger left linewidth; this asymmetry, well reproduced by the theory, has been observed in the experiments.[16]

In conclusion we used a novel formulation of the Raman scattering, permitting the simultaneous calculation of the absolute intensity, peak position, and linewidth. The present model is in fair agreement with microscopic theory[5] for what concerns the redshift. The comparison with the experiments, although qualitatively good, can still be improved including the specific experimental size dispersion.

*Electronic address: Giuseppe.Faraci@ct.infn.it

[1] M. Ehbrecht, H. Ferkel, F. Huisken, L. Holz, Yu. N. Polivanov, V. V. Smirnov, O. M. Steimakh, and R. Schmidt, J. Appl. Phys. **78**, 5302 (1995).

[2] M. Ehbrecht, B. Kohn, F. Huisken, M. A. Laguna, and V. Paillard, Phys. Rev. B **56**, 6958 (1997).

[3] V. Paillard, P. Puech, M. A. Laguna, R. Carles, B. Kohn, and F. Huisken, J. Appl. Phys. **86**, 1921 (1999).

[4] Hua Xia, Y. L. He, L. C. Wang, W. Zhang, X. N. Liu, X. K. Zhang, D. Fang, and Howard E. Jackson, J. Appl. Phys. **78**, 6705 (1995).

[5] Wei Cheng and Shang-Fen Ren, Phys. Rev. B **65**, 205305 (2002).

[6] Jian Zi, Kaiming Zhang, and Xide Xie, Phys. Rev. B **55**, 9263 (1997).

[7] Jian Zi, H. Büscher, C. Falter, W. Ludwig, Kaiming Zhang, and Xide Xie, Appl. Phys. Lett. **69**, 200 (1996).

[8] Takafumi Seto, Takaaki Orii, Maroto Hirasawa, and Nobuhiro Aya, Thin Solid Films **437**, 230 (2003).

[9] M. Perego, S. Ferrari, M. Fanciulli, G. Ben Assayag, C. Bonafos, M. Carrada, and A. Claverie, J. Appl. Phys. **95**, 257 (2004).

[10] H. Richter, Z. P. Wang, and L. Ley, Solid State Commun. **39**, 625 (1981).

[11] A. R. Pennisi, P. Russo, S. Gibilisco, G. Compagnini, S. Battiato, R. Puglisi, S. La Rosa, and G. Faraci, in *Progress in Condensed Matter Physics*, Conference Proc. Vol. 84, edited by G. Mondio and L. Silipigni (SIF, Bologna, 2003), p. 183; Eur. Phys. J. B **46**, 457 (2005).

[12] Y. Guyot, B. Champagnon, M. Boudeulle, P. Mélinon, B. Prével, v. Dupuis, and A. Perez, Thin Solid Films **297**, 188 (1997).

[13] Z. Igbal, S. Veprek, A. P. Webb, and P. Capezzuto, Solid State Commun. **37**, 993 (1981).

[14] Minoru Fujii, Yoshihiko Kanzawa, Shinji Hayashi, and Keiichi Yamamoto, Phys. Rev. B **54**, R8373 (1996).

[15] G. H. Li, K. Ding, Y. Chen, H. X. Han, and Z. P. Wang, J. Appl. Phys. **88**, 1439 (2000).

[16] P. Parayanthal and Fred H. Pollak, Phys. Rev. Lett. **52**, 1822 (1984).

[17] J. H. Campbell and P. M. Fauchet, Solid State Commun. **58**, 739 (1986).

[18] A. A. Sirenko, J. R. Fox, I. A. Akimov, X. X. Xi, S. Rumirov, and Z. Liliental-Weber, Solid State Commun. **113**, 553 (2000).

[19] Peter Y. Yu and Manuel Cardona, *Fundamentals of Semiconductors* (Springer, Berlin, 1996).

[20] R. Tubino, L. Piseri, and G. Zerbi, J. Chem. Phys. **56**, 1022 (1972).

[21] P. Melinon, P. Kéghelian, B. Prével, v. Dupuis, A. Perez, B. Champagnon, Y. Guyot, M. Pellarin, J. Lerné, M. Broyer, J. L. Rousset, and P. Delichére, J. Chem. Phys. **108**, 4607 (1998).

[22] P. Melinon, P. Kéghelian, B. Prével, A. Perez, J. Lerné, M. Pellarin, and M. Broyer, J. Chem. Phys. **107**, 10278 (1997).